Emergent c-axis magnetic helix in manganite-nickelate superlattices

G. Fabbris, N. Jaouen, D. Meyers, J. Feng, J. D. Hoffman, R. Sutarto, S. G. Chiuzbăian, A. Bhattacharya, and M. P. M. Dean

Phys. Rev. B **98**, 180401 — Published 2 November 2018

DOI: 10.1103/PhysRevB.98.180401

Emergent c-axis magnetic helix in manganite-nickelate superlattices

G. Fabbris,[1,2,*] N. Jaouen,[3] D. Meyers,[1] J. Feng,[4,†] J. D. Hoffman,[5,6,‡] R. Sutarto,[7] S. G. Chiuzbăian,[4,3] A. Bhattacharya,[5,6] and M. P. M. Dean[1,§]

[1]*Department of Condensed Matter Physics and Materials Science, Brookhaven National Laboratory, Upton, New York 11973, USA*
[2]*Advanced Photon Source, Argonne National Laboratory, Argonne, Illinois 60439, USA*
[3]*Synchrotron SOLEIL, L'Orme des Merisiers, Saint-Aubin, BP 48, 91192 Gif-sur-Yvette, France*
[4]*Sorbonne Université, CNRS, Laboratoire de Chimie Physique-Matiére et Rayonnement, UMR 7614, 4 place Jussieu, 75252 Paris Cedex 05, France*
[5]*Materials Science Division, Argonne National Laboratory, Argonne, Illinois 60439, USA*
[6]*Nanoscience and Technology Division, Argonne National Laboratory, Argonne, Illinois 60439, USA*
[7]*Canadian Light Source, Saskatoon, Saskatchewan S7N 2V3, Canada*

(Dated: October 10, 2018)

The nature of the magnetic order in $(La_{2/3}Sr_{1/3}MnO_3)_9/(LaNiO_3)_3$ superlattices is investigated using x-ray resonant magnetic reflectometry. We observe a new c-axis magnetic helix state in the $(LaNiO_3)_3$ layers that had never been measured in nickelates, and which mediates the $\sim 130^\circ$ magnetic coupling between the ferromagnetic $(La_{2/3}Sr_{1/3}MnO_3)_9$ layers, illustrating the power of x-rays for discovering the magnetic state of complex oxide interfaces. Resonant inelastic x-ray scattering and x-ray absorption spectroscopy show that Ni-O ligand hole states from bulk $LaNiO_3$ are mostly filled due to interfacial electron transfer from Mn, driving the Ni orbitals closer to an atomic-like $3d^8$ configuration. We discuss the constraints imposed by this electronic configuration to the microscopic origin of the observed magnetic structure. The presence of a magnetic helix in $(La_{2/3}Sr_{1/3}MnO_3)_9/(LaNiO_3)_3$ is crucial for modeling the potential spintronic functionality of this system and may be important for designing emergent magnetism in novel devices in general.

Interfaces between complex oxide materials exhibit remarkably rich physics driven by the interplay of various types of charge, orbital and spin couplings [1–3]. Particularly fascinating is their proven ability to host new types of emergent magnetic order that do not exist in either of the bulk constituents, representing a challenge to our understanding of electron correlations, as well as an opportunity for exploitation in spintronic devices [2–4]. In fact, complex magnetic phases are potentially common in transition metal oxide superlattices given the severe effects of interfacial symmetry breaking in localized $3d$ orbitals [5–10], but scrutiny over the microscopic magnetic interactions at such interfaces is often constrained by limited direct evidence of the resulting magnetic structure. Superlattices composed of manganites and nickelates are a paradigmatic venue for efforts to discover and understand emergent interface magnetism, motivated by the complex magnetic order and phase diagram of its bulk constituents [11, 12]. In fact, this system harbors fascinating phenomena, such as exchange bias and interfacial electronic reconstructions [13–27]. Recently, a highly unusual magnetic coupling between ferromagnetic $(LSMO)_9$ layers was observed in [001]-oriented $(La_{2/3}Sr_{1/3}MnO_3)_9/(LaNiO_3)_n$ $[(LSMO)_9/(LNO)_n, n = 1-9]$, in which the coupling angle between $(LSMO)_9$ layers varies between zero and 130° as a function of n (Fig. 1) [22]; an observation that, based on conceptual arguments, was suggestive of a magnetic helix in the $(LNO)_n$ layers. Despite the demonstrated ability of this system to be used as resistive memory devices [4], there is no experimental evidence for how or if the non-collinear magnetism of the $(LSMO)_9$ layers is mediated through $(LNO)_n$. Such lack of information critically hampers the ability to understand the physical mechanism driving the $(LSMO)_9$ magnetic coupling, which consequently inhibits the design of new superlattices with optimized magnetic properties.

In this work we focus on the $(LSMO)_9/(LNO)_3$ superlattice because it displays the largest magnetic coupling angle between the manganite layers ($\gamma \approx 130^\circ$ at 25 K [22]). We probe its magnetic and electronic structure using resonant soft x-ray techniques. The magnetic structure of both $(LSMO)_9$ and $(LNO)_3$ are studied using Mn and Ni L-edge x-ray resonant magnetic reflectivity (XRMR). We find that the nickelate layers contain a magnetic helix in which the Ni moments are mostly confined to the basal plane and rotate around the c-axis. Such magnetic structure is not present in any simple perovskite nickelate nor manganite. The XRMR ability to provide a precise description of the $(LSMO)_9/(LNO)_3$ magnetic ordering allows for a careful analysis of the magnetic interactions in this system. To this end, the nature of the Ni $3d$ and O $2p$ orbitals is probed through Ni L_3-edge resonant inelastic x-ray scattering (RIXS) and O K-edge x-ray absorption spectroscopy (XAS) measurements. The RIXS spectra are composed of well defined orbital excitations, which are reproduced by a model of localized Ni $3d^8$ orbitals under the effect of an octahedral crystal field. Even though the Ni $3d$ orbital is predominantly localized, O K-edge XAS show a small Ni $3d$ - O $2p$ ligand hole concentration, indicating that the NiO_2 planes are lightly hole-doped. While further work is

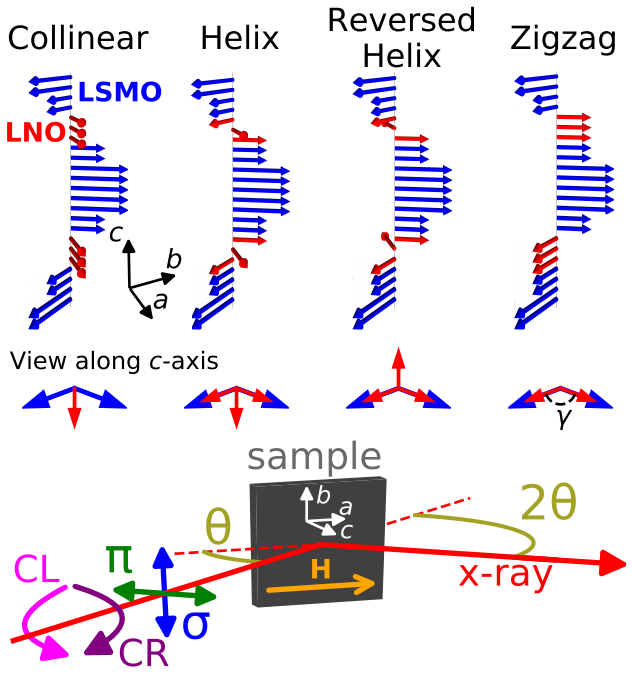

FIG. 1. Top & Middle: Possible magnetic structures of the $LaNiO_3$ layer in $(LSMO)_9/(LNO)_3$. The coupling angle γ corresponds to the angle between two $(LSMO)_9$ layers. Bottom: Experimental geometry used in both XRMR and RIXS measurements. XRMR was measured using circular and linear x-ray polarization with the magnetic field (H) applied along the sample's a-axis. RIXS was measured using linear x-ray polarization with θ and 2θ fixed to 15° and 85°, respectively.

needed to elucidate the magnetic couplings acting in this system, our analysis suggests that the $(LSMO)_9/(LNO)_3$ magnetic helix emerges from a combination between the strong pinning of Ni and Mn moments at the interfaces with a spin density wave (SDW) instability within the $(LNO)_3$ layers.

High-quality $14\times[(LSMO)_9/(LNO)_3]$ superlattices were grown on [001] single-crystalline $SrTiO_3$ substrates using molecular beam epitaxy as described previously [22, 28]. XRMR measurements were performed at the Ni and Mn L-edges [28] at the REIXS beamline of the Canadian Light Source [35] and at the SEXTANTS beamline of the SOLEIL synchrotron [36]. Data were collected using horizontal scattering geometry, as well as both linear (σ and π) and circular [left (CL) and right (CR)] x-ray polarizations (Fig. 1). Magnetic field was applied parallel to the sample surface and within the scattering plane using permanent magnets at REIXS and an electromagnet at SEXTANTS. In the former the data was collected at remanence after removing a 600 mT field, while in the later the sample was field cooled, and measured, under 1.2 mT. The temperature was kept at ∼25 K throughout the experiments. Data analysis was performed with the Dyna [37] and ReMagX [38] softwares using the magnetic matrix formalism. Resonant optical constants were obtained by combining the tabulated values with averaged XAS and x-ray magnetic circular dichroism measurements [28, 39].

Figure 2 displays a summary of the XRMR data collected on $(LSMO)_9/(LNO)_3$. The XRMR signal measured with circular light is primarily sensitive to components of the magnetization of each layer along the x-ray direction, while π polarization probes the transverse magnetization, and σ polarization is dominated by the lattice response [37, 38]. It is thus clear in Figs. 2 (a) through (d) that magnetic peaks appear at 1/2 order positions in $(LSMO)_9/(LNO)_3$ at both Mn and Ni edges indicating that the magnetic structure unit cell along the c-axis has twice the length of the chemical repetition. This observation is further demonstrated by the disappearance of such magnetic peaks when a field of 0.6 T is

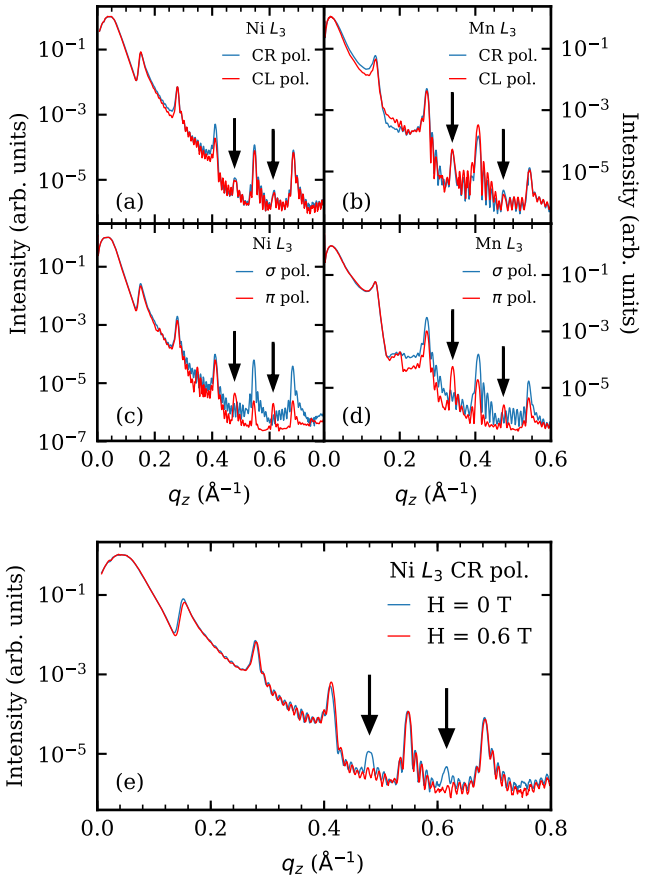

FIG. 2. (a)&(c) Ni L_3-edge (853.6 eV) XRMR data using circular and linear polarization, respectively. (b)&(d) Mn L_3-edge (641 eV) XRMR data using circular and linear polarization respectively. Data from both edges show half-order magnetic peaks (black arrows). This is consistent with a non-collinear magnetic structure between both LNO layers and LSMO layers as shown in Fig. 1. (e) Field dependence of the Ni L_3 XRMR data. A field of 0.6 T is sufficient to force a ferromagnetic alignment between every layer, which suppresses the half-order peaks, consistent with previous results [22].

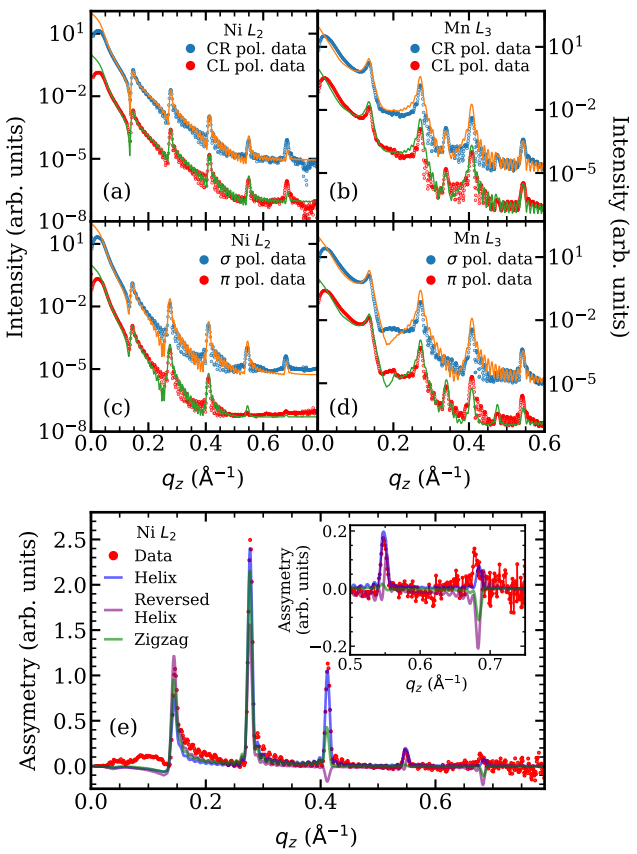

FIG. 3. Fits to the XRMR signal at the Ni L_2 (871.6 eV) [(a)&(c)] and Mn L_3 [(b)&(d)] edges in $(LSMO)_9/(LNO)_3$. Different polarization channels CR/CL or σ/π are shown as blue/red points and are overlapped by orange/green lines representing the fit. Different channels are offset from one another for clarity. Panel (e) displays the XRMR asymmetry [42]; the helix model is consistent with the presence of peaks at high q_z.

applied, which is sufficient to saturate the magnetic moments along the field [Fig. 2(e)] [22]. While the Mn edge results are consistent with the previous report [22], the data at the Ni edge indicates that a non-collinear magnetic structure is also present in the $(LNO)_3$ layer. Additionally, the simple presence of a magnetic response in the CR/CL XRMR demonstrates that there is a net magnetic moment in the NiO_2 planes [40]. Consequently, the magnetic structure of $(LNO)_3$ is different from the $(\frac{1}{4}\frac{1}{4}\frac{1}{4})$-type observed in [111]-grown LNO heterostructures and bulk $RENiO_3$ as this structure would lead to a zero net moment in the NiO_2 planes [23, 41]. However, this in itself does not distinguish between other $(LNO)_3$ magnetic structures such as the zigzag and (reversed) helical models (Fig. 1).

The $(LNO)_3$ and $(LSMO)_9$ magnetic structures are determined by modeling the XRMR data as shown in Fig. 3. Details of the modeling are provided in the Supplemental Materials [28]. The $(LSMO)_9$ magnetic structure obtained through the Mn L_3 edge XRMR modelling is consistent with previous results [28], thus we focus here on capturing the $(LNO)_3$ magnetic structure that could not be determined through neutron reflectivity [22]. Fits were performed at the Ni L_2-edge because there is a substantial overlap between the La M_4- and Ni L_3-edges, which makes the XRMR data analysis very difficult. Despite its magnetic sensitivity, the XRMR signal is largely dominated by charge responses [Fig. 3(a)-(d)]. In fact, the disagreements between simulation and experimental data seen at the Mn L_3-edge are at least partially driven by the expected $Mn^{4+/3+}$ valence modulation within the $(LSMO)_9$ layer [17, 22, 43]. We can overcome this challenge by isolating the magnetic response using the XRMR circular polarization asymmetry shown in Fig. 3(e) [42]. It is clear that only the helical model is able to reproduce all features in the data, particularly at high-q_z. Magnetic models with LNO spins away from the basal plane are not shown here but were also unable to reproduce the experimental data [28]. Modeling of both Mn and Ni edges is consistent with $\gamma = 140(20)^\circ$ in agreement with neutron reflectivity [22, 44]. The $(LNO)_3$ c-axis magnetic helix result is surprising as such structures are uncommon in bulk transition metal oxides and have not previously been observed in nickelates. This demonstrates that in $(LSMO)_9/(LNO)_3$ the interfacial symmetry breaking and charge transfer drive an emergent form of magnetism, the underlying electronic structure of which we now explore.

We first address the character of the nickelate layer $3d$ orbital using Ni L_3-edge RIXS. Data was collected at 30 K using the AERHA end-station of the SEXTANTS beamline at the SOLEIL synchrotron [48]. The experimental scattering geometry is detailed in Fig. 1. Figure 4 shows the RIXS spectra as a function of incident x-ray energy and linear polarization. The experimental data [Fig. 4 (a)&(b)] is composed of narrow peaks that are consistent with dispersionless localized orbital excitations of $3d^8$ (Ni^{2+}) ions [47, 49–51]; a distinctively different broad diagonal feature is seen in RIXS spectra of bulk $RENiO_3$ and hole-doped $La_{2-x}Sr_xNiO_4$ (for $x \geq 1/3$) [47, 51, 52], in which the significant amount of extra holes in the NiO_2 plane populate the hybridized Ni $3d$ - O $2p$ ligand hole states. This result is consistent with Ni L_2-edge XAS data [22]. The RIXS spectra was simulated using the Kramers-Heisenberg equation combined with atomic multiplet calculations performed with the Cowan and RACER codes [45–47]. These simulations [Fig. 4 (c)&(d)] nicely reproduce the observed signal [28], confirming that these are orbital dd excitations, thus demonstrating the localized character of the Ni $3d$ state in $(LSMO)_9/(LNO)_3$. Furthermore, the excellent agreement between experimental data and simulation implies high-spin ($S = 1$) Ni $3d^8$ orbitals under a nearly octahedral crystal field with $10D_q = 1.1$ eV and $\Delta e_g = 0.05$ eV [53].

While the RIXS results establish a predominantly lo-

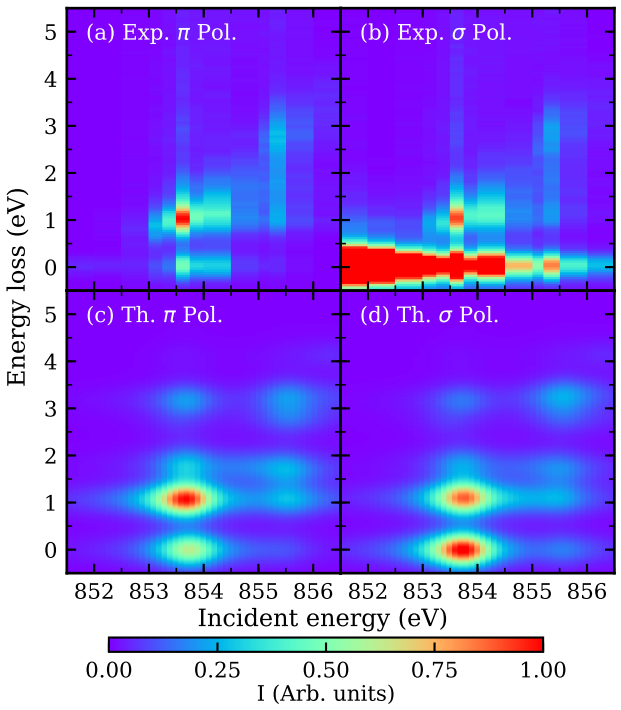

FIG. 4. Ni L_3-edge RIXS of $(LSMO)_9/(LNO)_3$. Data for π and σ polarized incident x-rays are displayed in panels (a)&(b), respectively. Panels (c)&(d) present simulations of the RIXS spectra for π and σ polarization using atomic calculations [45–47].

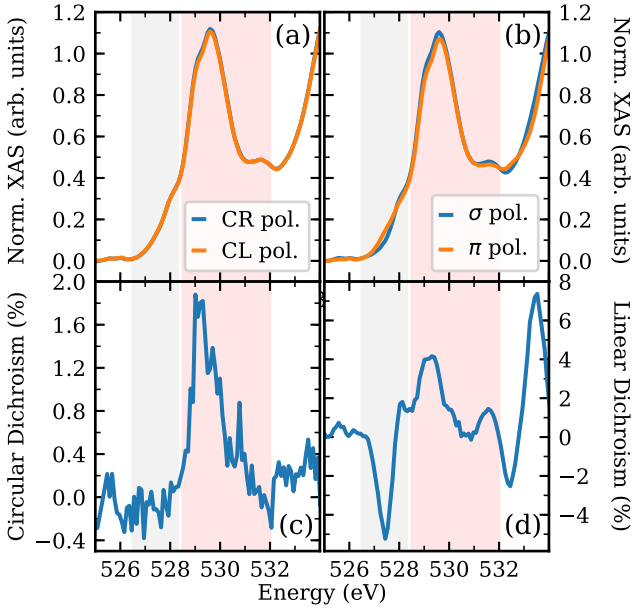

FIG. 5. $(LSMO)_9/(LNO)_3$ O K-edge XAS data. (a)&(b) show the pre-edge features of the XAS collected with circular and linear x-rays, respectively. The circular and linear dichroism are plotted in panels (c)&(d), respectively. While signal from hybridized Mn-O orbitals dominate the pre-edge features (red box), a signal that is consistent with Ni-O hybridization is seen around 527.4 eV (grey box).

calized Ni $3d$ orbital, it has minimal sensitivity to the potential presence of a small amount of Ni $3d$ - O $2p$ ligand holes. Figure 5 displays the pre-edge of the O K-edge XAS data collected in total electron yield mode at the REIXS beamline of the Canadian Light Source. The x-rays were incident at 15° and the sample was field cooled to 25 K under 0.6 T, but the magnetic field was removed prior to the data collection. The pre-edge is dominated by features related to Mn-O and Ni-O ligand holes. Comparing this data with the literature [54, 55], it is clear that the Mn-O states dominate the signal (red box). This result is consistent with the large response expected for Mn $3d^4/3d^3$ ($Mn^{3+/4+}$) and small or absent pre-edge structure for Ni near the $3d^8$ state (Ni^{2+}) [56–58]. It is also consistent with the position of the magnetic circular dichroism signal, which is expected to be dominated by LSMO [Fig. 5(a)&(c)]. However, a small pre-edge shoulder is seen at an energy that is consistent with it originating in the LNO layer (grey box). Interestingly this feature displays a marked linear dichroism [defined here as the XAS (σ pol.) - XAS (π pol.)], implying an anisotropic ligand hole state in which the more holes populate the $3d_{3z^2-r^2}2p_z$ states in detriment of $3d_{x^2-y^2}2p_\sigma$. This result is consistent with the tensile strain applied by the $SrTiO_3$ substrate and is in-line with the concept that strain primarily controls the Ni-O hybridization in LNO heterostructures [47, 59, 60].

We now discuss the consequences of the observed electronic configuration to the potential mechanisms driving the complex magnetic structure of $(LSMO)_9/(LNO)_3$. We start by noting that non-collinear magnetic order in transition metal oxides may derive from the Dzyaloshinskii-Moriya interaction [61, 62], but this interaction is inconsistent with the symmetry of the $(LNO)_3$ magnetic structure [22]. The interfacial electronic reconstruction in $(LSMO)_9/(LNO)_3$ induces magnetic frustration in the nickelate layer since the antiferromagnetic Ni^{2+}-O-Ni^{2+} exchange energy is expected to be similar to the dominant ferromagnetic Ni^{2+}-O-Mn^{4+} [18, 51, 63, 64]. However, while we cannot exclude frustration as the sole reason for the observed spiral, if we only consider first neighbor interactions, such frustration would arguably drive an antiferromagnetic structure that resembles the reversed helical model (see Fig. 1) since the adjacent NiO_2 planes would favor an antiferromagnetic coupling. Additionally, it is difficult to reconcile the magnetic structure LNO thickness dependence with a magnetic frustration model [22]. Emergent magnetic phenomena are often seen in systems that, much like $(LSMO)_9/(LNO)_3$, have $3d$-$2p$ ligand holes (negative charge transfer systems [65]), including certain cuprates [66], hole-doped La_2NiO_4 [51, 57], $RENiO_3$ [52], and CrO_2 [67]. In fact, it has been argued that double-

exchange and superexchange can act together to create non-collinear canted structures in such systems [68–70], but it is not entirely clear how such canting would actually lead to a helix. Finally, we note that the electronic structure of $(LNO)_3$ closely mimics that of lightly hole-doped La_2NiO_4 [51, 57, 71, 72], which displays stripe-like spin density wave instabilities [73, 74], which in turn are known to foster non-collinear magnetic structures [75, 76]. Therefore, it appears that the $(LNO)_3$ magnetic helix emerges from the coupling of such SDW instability with the interfacial Ni-Mn interaction.

In conclusion, the presence of an emergent magnetic helical structure in the $[La_{2/3}Sr_{1/3}MnO_3]_9/[LaNiO_3]_3$ superlattice is demonstrated through XRMR measurements. Such c-axis magnetic helix has not been shown to occur in any other nickelate system. Ni L_3-edge RIXS and O K-edge XAS experiments show that interfacial charge transfer results in NiO_2 planes with lightly hole-doped Ni $3d^8$ atoms. We argue that such electronic structure likely drives SDW instabilities that may drive the helical magnetic structure, but further work is required to verify our arguments. Besides theoretical investigations, we believe that the role of octahedral rotations in this system need to be addressed as these are known to relevant to magnetic exchange. Nevertheless, the prospect of engineering spin density waves through interfaces to create novel magnetism is tantalizing, and, in principle, such approach should applicable to the various families of negative charge transfer transition metal oxides [65].

We thank Dr. Daniel Haskel for insightful discussions and Dr. Alessandro Nicolaou for support during the RIXS measurements at the SEXTANTS beamline. This material is based upon work supported by the U.S. Department of Energy, Office of Basic Energy Sciences, Early Career Award Program under Award Number 1047478. Work at Brookhaven National Laboratory is supported by the U.S. Department of Energy, Office of Science, Office of Basic Energy Sciences, under Contract No. DE-SC0012704. Work at Argonne is supported by the U.S. Department of Energy, Office of Science, under contract No. DE-AC-02-06CH11357. Part of the research described in this paper was performed at the Canadian Light Source, which is supported by the Canada Foundation for Innovation, Natural Sciences and Engineering Research Council of Canada, the University of Saskatchewan, the Government of Saskatchewan, Western Economic Diversification Canada, the National Research Council Canada, and the Canadian Institutes of Health Research. We acknowledge SOLEIL for provision of synchrotron radiation facilities. S.G.C. acknowledges the support of the Agence Nationale de la Recherche (ANR), under Grant No. ANR-05-NANO-074 (HR-RXRS).

* gfabbris@anl.gov
† Present address: CAS Key Laboratory of Magnetic Materials and Devices, Ningbo Institute of Materials Technology and Engineering, Chinese Academy of Sciences, Zhejiang 315201 Ningbo, China
‡ Present address: Department of Physics, Harvard University, Cambridge, MA 02138, USA
§ mdean@bnl.gov

[1] Pavlo Zubko, Stefano Gariglio, Marc Gabay, Philippe Ghosez, and Jean-Marc Triscone, "Interface Physics in Complex Oxide Heterostructures," Annual Review of Condensed Matter Physics **2**, 141–165 (2011).
[2] Anand Bhattacharya and Steven J. May, "Magnetic Oxide Heterostructures," Annual Review of Materials Research **44**, 65–90 (2014).
[3] Frances Hellman, Axel Hoffmann, Yaroslav Tserkovnyak, Geoffrey S. D. Beach, Eric E Fullerton, Chris Leighton, Allan H. MacDonald, Daniel C Ralph, Dario A. Arena, Hermann A. Dürr, Peter Fischer, Julie Grollier, Joseph P. Heremans, Tomas Jungwirth, Alexey V. Kimel, Bert Koopmans, Ilya N. Krivorotov, Steven J. May, Amanda K. Petford-Long, James M. Rondinelli, Nitin Samarth, Ivan K. Schuller, Andrei N. Slavin, Mark D. Stiles, Oleg Tchernyshyov, André Thiaville, and Barry L. Zink, "Interface-induced phenomena in magnetism," Reviews of Modern Physics **89**, 025006 (2017).
[4] Jason D. Hoffman, Stephen M. Wu, Brian J. Kirby, and Anand Bhattacharya, "Tunable Noncollinear Antiferromagnetic Resistive Memory through Oxide Superlattice Design," Physical Review Applied **9**, 044041 (2018).
[5] Sumilan Banerjee, Onur Erten, and Mohit Randeria, "Ferromagnetic exchange, spin-orbit coupling and spiral magnetism at the $LaAlO_3/SrTiO_3$ interface," Nature Physics **9**, 626–630 (2013).
[6] Xiaopeng Li, W. V. Liu, and Leon Balents, "Spirals and Skyrmions in Two Dimensional Oxide Heterostructures," Physical Review Letters **112**, 067202 (2014).
[7] Sergej Fust, Saumya Mukherjee, Neelima Paul, Jochen Stahn, Wolfgang Kreuzpaintner, Peter Böni, and Amitesh Paul, "Realizing topological stability of magnetic helices in exchange-coupled multilayers for all-spin-based system," Scientific Reports **6**, 33986 (2016).
[8] Pouya Moetakef, James R. Williams, Daniel G. Ouellette, Adam P. Kajdos, David Goldhaber-Gordon, S. J. Allen, and Susanne Stemmer, "Carrier-Controlled Ferromagnetism in $SrTiO_3$," Physical Review X **2**, 021014 (2012).
[9] A. Brinkman, M. Huijben, M. van Zalk, J. Huijben, U. Zeitler, J. C. Maan, W. G. van der Wiel, G. Rijnders, D. H. A. Blank, and H. Hilgenkamp, "Magnetic effects at the interface between non-magnetic oxides," Nature Materials **6**, 493–496 (2007).
[10] M. Hepting, R. J. Green, Z. Zhong, M. Bluschke, Y. E. Suyolcu, S. Macke, A. Frano, S. Catalano, M. Gibert, R. Sutarto, F. He, G. Cristiani, G. Logvenov, Y. Wang, P. A. van Aken, P. Hansmann, M. Le Tacon, J.-M. Triscone, G. A. Sawatzky, B. Keimer, and E. Benckiser, "Complex magnetic order in nickelate slabs," Nature Physics (2018), 10.1038/s41567-018-0218-5.
[11] Clarence Zener, "Interaction between the d-Shells in the Transition Metals. II. Ferromagnetic Compounds of Man-

ganese with Perovskite Structure," Physical Review **82**, 403–405 (1951).

[12] J. B. Torrance, P. Lacorre, A. I. Nazzal, E. J. Ansaldo, and Ch. Niedermayer, "Systematic study of insulator-metal transitions in perovskites $RNiO_3$ (R=Pr,Nd,Sm,Eu) due to closing of charge-transfer gap," Physical Review B **45**, 8209–8212 (1992).

[13] K. R. Nikolaev, A. Bhattacharya, P. A. Kraus, V. A. Vas'ko, W. K. Cooley, and A. M. Goldman, "Indications of antiferromagnetic interlayer coupling in $La_{2/3}Ba_{1/3}MnO_3/LaNiO_3$ multilayers," Applied Physics Letters **75**, 118–120 (1999).

[14] K. R. Nikolaev, A. Y. Dobin, I. N. Krivorotov, W. K. Cooley, A. Bhattacharya, A. L. Kobrinskii, L. I. Glazman, R. M. Wentzovitch, E. D. Dahlberg, and A. M. Goldman, "Oscillatory Exchange Coupling and Positive Magnetoresistance in Epitaxial Oxide Heterostructures," Physical Review Letters **85**, 3728–3731 (2000).

[15] J. C. Rojas Sánchez, B. Nelson-Cheeseman, M. Granada, E. Arenholz, and L. B. Steren, "Exchange-bias effect at $La_{0.75}Sr_{0.25}MnO_3/LaNiO_3$ interfaces," Physical Review B **85**, 094427 (2012).

[16] Marta Gibert, Pavlo Zubko, Raoul Scherwitzl, Jorge Íñiguez, and Jean-Marc Triscone, "Exchange bias in $LaNiO_3 - LaMnO_3$ superlattices," Nature Materials **11**, 195–198 (2012).

[17] J. Hoffman, I. C. Tung, B. B. Nelson-Cheeseman, M. Liu, J. W. Freeland, and A. Bhattacharya, "Charge transfer and interfacial magnetism in $(LaNiO_3)_n/(LaMnO_3)_2$ superlattices," Physical Review B **88**, 144411 (2013).

[18] Alex Taekyung Lee and Myung Joon Han, "Charge transfer, confinement, and ferromagnetism in $LaMnO_3/LaNiO_3$ (001) superlattices," Physical Review B **88**, 035126 (2013).

[19] M. Gibert, M. Viret, A. Torres-Pardo, C. Piamonteze, P. Zubko, N. Jaouen, J.-M. Tonnerre, A. Mougin, J. Fowlie, S. Catalano, A. Gloter, O. Stéphan, and J.-M. Triscone, "Interfacial Control of Magnetic Properties at $LaMnO_3/LaNiO_3$ Interfaces," Nano Letters **15**, 7355–7361 (2015).

[20] C. Piamonteze, M. Gibert, J. Heidler, J. Dreiser, S. Rusponi, H. Brune, J.-M. Triscone, F. Nolting, and U. Staub, "Interfacial properties of $LaMnO_3/LaNiO_3$ superlattices grown along (001) and (111) orientations," Physical Review B **92**, 014426 (2015).

[21] Xingkun Ning, Zhanjie Wang, and Zhidong Zhang, "Fermi Level shifting, Charge Transfer and Induced Magnetic Coupling at $La_{0.7}Ca_{0.3}MnO_3/LaNiO_3$ Interface," Scientific Reports **5**, 8460 (2015).

[22] Jason D. Hoffman, Brian J. Kirby, Jihwan Kwon, Gilberto Fabbris, D. Meyers, John W. Freeland, Ivar Martin, Olle G. Heinonen, Paul Steadman, Hua Zhou, Christian M. Schlepütz, Mark P. M. Dean, Suzanne G. E. te Velthuis, Jian-Min Zuo, and Anand Bhattacharya, "Oscillatory Noncollinear Magnetism Induced by Interfacial Charge Transfer in Superlattices Composed of Metallic Oxides," Physical Review X **6**, 041038 (2016).

[23] M. Gibert, M. Viret, P. Zubko, N. Jaouen, J.-M. Tonnerre, A. Torres-Pardo, S. Catalano, A. Gloter, O. Stéphan, and J.-M. Triscone, "Interlayer coupling through a dimensionality-induced magnetic state," Nature Communications **7**, 11227 (2016).

[24] Miho Kitamura, Koji Horiba, Masaki Kobayashi, Enju Sakai, Makoto Minohara, Taichi Mitsuhashi, Atsushi Fujimori, Takuro Nagai, Hiroshi Fujioka, and Hiroshi Kumigashira, "Spatial distribution of transferred charges across the heterointerface between perovskite transition metal oxides $LaNiO_3$ and $LaMnO_3$," Applied Physics Letters **108**, 111603 (2016).

[25] Julu Zang, Guowei Zhou, Yuhao Bai, Zhiyong Quan, and Xiaohong Xu, "The Exchange Bias of $LaMnO_3/LaNiO_3$ Superlattices Grown along Different Orientations," Scientific Reports **7**, 10557 (2017).

[26] C. L. Flint, A. Vailionis, H. Zhou, H. Jang, J.-S. Lee, and Y. Suzuki, "Tuning interfacial ferromagnetism in $LaNiO_3/CaMnO_3$ superlattices by stabilizing nonequilibrium crystal symmetry," Physical Review B **96**, 144438 (2017).

[27] C. L. Flint, H. Jang, J.-S. Lee, A. T. N'Diaye, P. Shafer, E. Arenholz, and Y. Suzuki, "Role of polar compensation in interfacial ferromagnetism of $LaNiO_3$ superlattices," Physical Review Materials **1**, 024404 (2017).

[28] See Supplemental Material at [URL] for information on the sample characterization, Mn, Ni L-edge, and O K-edge x-ray absorption spectroscopy data, as well as further details on the atomic simulation of the Ni L-edge resonant inelastic x-ray scattering data, which includes Refs. [20, 22, 29–34, 37–39, 47, 51, 52].

[29] Jorge E Hamann-Borrero, Sebastian Macke, Woo Seok Choi, Ronny Sutarto, Feizhou He, Abdullah Radi, Ilya Elfimov, Robert J Green, Maurits W Haverkort, Volodymyr B Zabolotnyy, Ho Nyung Lee, George A Sawatzky, and Vladimir Hinkov, "Valence-state reflectometry of complex oxide heterointerfaces," npj Quantum Materials **1**, 16013 (2016).

[30] J. van Elp, B. G. Searle, G. A. Sawatzky, and M. Sacchi, "Ligand hole induced symmetry mixing of d^8 states in $Li_xNi_{1x}O$, as observed in Ni $2p$ x-ray absorption spectroscopy," Solid State Communications **80**, 67–71 (1991).

[31] M. Abbate, F. M. F. de Groot, J. C. Fuggle, A. Fujimori, Y. Tokura, Y. Fujishima, O. Strebel, M. Domke, G. Kaindl, J. van Elp, B. T. Thole, G. A. Sawatzky, M. Sacchi, and N. Tsuda, "Soft-x-ray-absorption studies of the location of extra charges induced by substitution in controlled-valence materials," Physical Review B **44**, 5419–5422 (1991).

[32] C. Aruta, G. Ghiringhelli, V. Bisogni, L. Braicovich, N. B. Brookes, A. Tebano, and G. Balestrino, "Orbital occupation, atomic moments, and magnetic ordering at interfaces of manganite thin films," Physical Review B **80**, 014431 (2009).

[33] Paolo Carra, B. T. Thole, Massimo Altarelli, and Xindong Wang, "X-ray circular dichroism and local magnetic fields," Physical Review Letters **70**, 694–697 (1993).

[34] Haizhong Guo, Arunava Gupta, Maria Varela, Stephen Pennycook, and Jiandi Zhang, "Local valence and magnetic characteristics of La_2NiMnO_6," Physical Review B **79**, 172402 (2009).

[35] D. G. Hawthorn, F. He, L. Venema, H. Davis, A. J. Achkar, J. Zhang, R. Sutarto, H. Wadati, A. Radi, T. Wilson, G. Wright, K. M. Shen, J. Geck, H. Zhang, V. Novk, and G. A. Sawatzky, "An in-vacuum diffractometer for resonant elastic soft x-ray scattering," Review of Scientific Instruments **82**, 073104 (2011).

[36] Nicolas Jaouen, Jean-Marc Tonnerre, Grigor Kapoujian, Pierre Taunier, Jean-Paul Roux, Denis Raoux, and Fausto Sirotti, "An apparatus for temperature-

dependent soft X-ray resonant magnetic scattering," Journal of Synchrotron Radiation **11**, 353–357 (2004).

[37] M. Elzo, E. Jal, O. Bunau, S. Grenier, Y. Joly, A. Y. Ramos, H. C. N. Tolentino, J. M. Tonnerre, and N. Jaouen, "X-ray resonant magnetic reflectivity of stratified magnetic structures: Eigenwave formalism and application to a W/Fe/W trilayer," Journal of Magnetism and Magnetic Materials **324**, 105–112 (2012).

[38] S. Macke and E. Goering, "Magnetic reflectometry of heterostructures," Journal of Physics: Condensed Matter **26**, 363201 (2014).

[39] C. T. Chantler, "Theoretical Form Factor, Attenuation, and Scattering Tabulation for Z =192 from E =110 eV to E =0.41.0 MeV," Journal of Physical and Chemical Reference Data **24**, 71–643 (1995).

[40] While we are unable to determine the magnetic structure within the NiO_2 planes, x-ray magnetic circular dichroism sum rules analysis suggests a canted antiferromagnetic coupling [28].

[41] V. Scagnoli, U. Staub, Y. Bodenthin, M. García-Fernández, A. M. Mulders, G. I. Meijer, and G. Hammerl, "Induced noncollinear magnetic order of Ni^{3+} in $NdNiO_3$ observed by resonant soft x-ray diffraction," Physical Review B **77**, 115138 (2008).

[42] The XRMR assymetry is defined here as the difference between right and left polarized XRMR times q_z^4.

[43] M. Zwiebler, J. E. Hamann-Borrero, M. Vafaee, P. Komissinskiy, S. Macke, R. Sutarto, F. He, B. Büchner, G. A. Sawatzky, L. Alff, and J. Geck, "Electronic depth profiles with atomic layer resolution from resonant soft x-ray reflectivity," New Journal of Physics **17**, 083046 (2015).

[44] We estimate the uncertainty on determining the in- and out-of-plane magnetic moment angles to be $\sim 20^\circ$ and $\sim 30^\circ$, respectively [28].

[45] R. D. Cowan, *The Theory of Atomic Structure and Spectra* (University of California Press, Berkeley, 1981).

[46] Frank De Groot and Akio Kotani, *Core level spectroscopy of solids* (CRC press, 2008).

[47] G. Fabbris, D. Meyers, J. Okamoto, J. Pelliciari, A. S. Disa, Y. Huang, Z. Y. Chen, W. B. Wu, C. T. Chen, S. Ismail-Beigi, C. H. Ahn, F. J. Walker, D. J. Huang, T. Schmitt, and M. P. M. Dean, "Orbital engineering in nickelate heterostructures driven by anisotropic oxygen hybridization rather than orbital energy levels," Physical Review Letters **117**, 147401 (2016).

[48] Sorin G. Chiuzbian, Coryn F. Hague, Antoine Avila, Renaud Delaunay, Nicolas Jaouen, Maurizio Sacchi, François Polack, Muriel Thomasset, Bruno Lagarde, Alessandro Nicolaou, Stefania Brignolo, Cédric Baumier, Jan Lüning, and Jean-Michel Mariot, "Design and performance of AERHA, a high acceptance high resolution soft x-ray spectrometer," Review of Scientific Instruments **85**, 043108 (2014).

[49] G Ghiringhelli, M Matsubara, C Dallera, F Fracassi, R Gusmeroli, A Piazzalunga, A Tagliaferri, N B Brookes, A Kotani, and L Braicovich, "NiO as a test case for high resolution resonant inelastic soft x-ray scattering," Journal of Physics: Condensed Matter **17**, 5397–5412 (2005).

[50] G. Ghiringhelli, A. Piazzalunga, C. Dallera, T. Schmitt, V. N. Strocov, J. Schlappa, L. Patthey, X. Wang, H. Berger, and M. Grioni, "Observation of Two Nondispersive Magnetic Excitations in NiO by Resonant Inelastic Soft-X-Ray Scattering," Physical Review Letters **102**, 027401 (2009).

[51] G. Fabbris, D. Meyers, L. Xu, V. M. Katukuri, L. Hozoi, X. Liu, Z.-Y. Chen, J. Okamoto, T. Schmitt, A. Uldry, B. Delley, G. D. Gu, D. Prabhakaran, A. T. Boothroyd, J. van den Brink, D. J. Huang, and M. P. M. Dean, "Doping Dependence of Collective Spin and Orbital Excitations in the Spin-1 Quantum Antiferromagnet $La_{2-x}Sr_xNiO_4$ Observed by X Rays," Physical Review Letters **118**, 156402 (2017).

[52] Valentina Bisogni, Sara Catalano, Robert J. Green, Marta Gibert, Raoul Scherwitzl, Yaobo Huang, Vladimir N. Strocov, Pavlo Zubko, Shadi Balandeh, Jean-Marc Triscone, George Sawatzky, and Thorsten Schmitt, "Ground-state oxygen holes and the metal-insulator transition in the negative charge-transfer rare-earth nickelates," Nature Communications **7**, 13017 (2016).

[53] Best agreement with the experimental data was obtained with $\Delta t_{2g} = 0$ and reduced Slater-Condon parameters: $F_{dd} = 70\%$, $F_{pd} = 85\%$ and $G_{pd} = 70\%$. We point out that the $\Delta e_g = 0.05$ eV found here implies that Δt_{2g} is likely finite. However, it also suggests a $\Delta t_{2g} < 0.01$ eV, which is smaller than our sensitivity.

[54] José M. Alonso, Raquel Cortés-Gil, Luisa Ruiz-González, José M. González-Calbet, Antonio Hernando, María Vallet-Regí, María E. Dávila, and María C. Asensio, "Influence of the Synthetic Pathway on the Properties of Oxygen-Deficient Manganese-Related Perovskites," European Journal of Inorganic Chemistry **2007**, 3350–3355 (2007).

[55] B. Cui, C. Song, F. Li, G. Y. Wang, H. J. Mao, J. J. Peng, F. Zeng, and F. Pan, "Tuning the entanglement between orbital reconstruction and charge transfer at a film surface," Scientific Reports **4**, 4206 (2015).

[56] P. Kuiper, D. E. Rice, D. J. Buttrey, H.-J. Lin, and C. T. Chen, "Isotropic O 1*s* prepeak as evidence for polarons in $La_2NiO_{4+\delta}$," Physica B: Condensed Matter **208-209**, 271–272 (1995).

[57] E. Pellegrin, J. Zaanen, H.-J. Lin, G. Meigs, C. T. Chen, G. H. Ho, H. Eisaki, and S. Uchida, "O 1*s* near-edge x-ray absorption of $La_{2-x}Sr_xNiO_{4+\delta}$: Holes, polarons, and excitons," Physical Review B **53**, 10667–10679 (1996).

[58] Yanwei Cao, Xiaoran Liu, M. Kareev, D. Choudhury, S. Middey, D. Meyers, J.-W. Kim, P. J. Ryan, J.W. Freeland, and J. Chakhalian, "Engineered Mott ground state in a $LaTiO_{3+\delta}/LaNiO_3$ heterostructure," Nature Communications **7**, 10418 (2016).

[59] N. Parragh, G. Sangiovanni, P. Hansmann, S. Hummel, K. Held, and A. Toschi, "Effective crystal field and Fermi surface topology: A comparison of *d*- and *dp*- orbital models," Physical Review B **88**, 195116 (2013).

[60] M. N. Grisolia, J. Varignon, G. Sanchez-Santolino, A. Arora, S. Valencia, M. Varela, R. Abrudan, E. Weschke, E. Schierle, J. E. Rault, J.-P. Rueff, A. Barthélémy, J. Santamaria, and M. Bibes, "Hybridization-controlled charge transfer and induced magnetism at correlated oxide interfaces," Nature Physics **12**, 484–492 (2016).

[61] I. Dzyaloshinsky, "A thermodynamic theory of weak ferromagnetism of antiferromagnetics," Journal of Physics and Chemistry of Solids **4**, 241–255 (1958).

[62] Tôru Moriya, "Anisotropic Superexchange Interaction and Weak Ferromagnetism," Physical Review **120**, 91–98 (1960).

[63] Kenji Nakajima, Kazuyoshi Yamada, Syoichi Hosoya, To-

moya Omata, and Yasuo Endoh, "Spin-wave excitations in two dimensional antiferromagnet of stoichiometric La_2NiO_4," Journal of the Physical Society of Japan **62**, 4438–4448 (1993).

[64] D. Haskel, G. Fabbris, N. M. Souza-Neto, M. van Veenendaal, G. Shen, A. E. Smith, and M. A. Subramanian, "Stability of the ferromagnetic ground state of La_2MnNiO_6 against large compressive stress," Physical Review B **84**, 100403 (2011).

[65] D. Khomskii, "Unusual valence, negative charge-transfer gaps and self-doping in transition-metal compounds," arXiv:0101164 [cond-mat].

[66] T. Mizokawa, H. Namatame, A. Fujimori, K. Akeyama, H. Kondoh, H. Kuroda, and N. Kosugi, "Origin of the band gap in the negative charge-transfer-energy compound $NaCuO_2$," Physical Review Letters **67**, 1638–1641 (1991).

[67] M. A. Korotin, V. I. Anisimov, D. I. Khomskii, and G. A. Sawatzky, "CrO_2: A Self-Doped Double Exchange Ferromagnet," Physical Review Letters **80**, 4305–4308 (1998).

[68] P. G. de Gennes, "Effects of Double Exchange in Magnetic Crystals," Physical Review **118**, 141–154 (1960).

[69] Maxim Mostovoy, "Helicoidal Ordering in Iron Perovskites," Physical Review Letters **94**, 137205 (2005).

[70] T. S. Santos, B. J. Kirby, S. Kumar, S. J. May, J. A. Borchers, B. B. Maranville, J. Zarestky, S. G. E. te Velthuis, J. van den Brink, and A. Bhattacharya, "Delta Doping of Ferromagnetism in Antiferromagnetic Manganite Superlattices," Physical Review Letters **107**, 167202 (2011).

[71] Pieter Kuiper, J. van Elp, D. E. Rice, D. J. Buttrey, H.-J. Lin, and C. T. Chen, "Polarization-dependent nickel $2p$ x-ray-absorption spectra of $La_2NiO_{4+\delta}$," Physical Review B **57**, 1552–1557 (1998).

[72] Based on comparing the Ni L_2 edge XAS and L_3 edge RIXS with the literature [30, 31, 51], we roughly estimate an average $\sim$0.1-0.3 holes/Ni in the $(LNO)_3$ layers.

[73] John M. Tranquada, D. J. Buttrey, V. Sachan, and J. E. Lorenzo, "Simultaneous Ordering of Holes and Spins in $La_2NiO_{4.125}$," Physical Review Letters **73**, 1003–1006 (1994).

[74] V. Sachan, D. J. Buttrey, J. M. Tranquada, J. E. Lorenzo, and G. Shirane, "Charge and spin ordering in $La_{2-x}Sr_xNiO_{4.00}$ with x=0.135 and 0.20," Physical Review B **51**, 12742–12746 (1995).

[75] Boris I. Shraiman and Eric D. Siggia, "Mobile Vacancies in a Quantum Heisenberg Antiferromagnet," Physical Review Letters **61**, 467–470 (1988).

[76] Oron Zachar, S. A. Kivelson, and V. J. Emery, "Landau theory of stripe phases in cuprates and nickelates," Physical Review B **57**, 1422–1426 (1998).